Spatio-temporal variability of tidal-stream energy in north-western Europe

Guillou, Nicolas; Neill, Simon; Thiebot, Jerome

Philosophical Transactions of the Royal Society A: Mathematical, Physical and Engineering Sciences

DOI:
10.1098/rsta.2019.0493

Published: 21/08/2020

Peer reviewed version

Research

Article submitted to journal

Subject Areas:
marine renewable energy, numerical modelling, tidal harmonic analysis, Telemac, ROMS

Keywords:
Alderney Race, Pentland Firth, Orkney, Fromveur Strait, EMEC, Fall of Warness

Author for correspondence:
Nicolas Guillou
e-mail: nicolas.guillou@cerema.fr

Spatio-temporal variability of tidal-stream energy in north-western Europe

Nicolas Guillou[1], Simon P. Neill[2] and Jérôme Thiébot[3]

[1]Laboratoire de Génie Côtier et Environnement (LGCE), Cerema, Directon Eau Mer et Fleuves, ER, 155 rue Pierre Bouguer, Technopôle Brest-Iroise, BP 5, 29280, Plouzané, France
[2]School of Ocean Sciences, Bangor University, LL59 5 AB, United-Kingdom
[3]Normandie University, UNICAEN, LUSAC, EA4253, Site universitaire de Cherbourg, rue Louis Aragon, BP 78, F-50130, Cherbourg-Octeville, France

Initial selection of tidal stream energy sites is primarily based on identifying areas with the maximum current speeds. However, optimal design and deployment of turbines requires detailed investigations of the temporal variability of the available resource, focusing on areas with reduced variability, and hence the potential for more continuous energy conversion. These aspects are investigated here for some of the most promising sites for tidal array development across the north-western European shelf seas: the Alderney Race, the Fromveur Strait, the Pentland Firth, and the Orkney channels. Particular attention was dedicated to asymmetry between the flood and ebb phases of the tidal cycle (due to the phase relationship between M_2 and M_4 constituents), and spring-neap variability of the available resource (due to M_2 and S_2 compound tides). A series of high resolution models were exploited to (i) produce a detailed harmonic database of these three components, and (ii) characterize, using energy resource metrics, temporal variability of the available power density. There was a clear contrast between the Alderney Race, with reduced temporal variability over semi-diurnal and fortnightly time scales, and sites in western Brittany and North Scotland which, due to increased variability, appeared less attractive for optimal energy conversion.

1. Introduction

Exploitation of the hydro-kinetic power of tidal currents by in-stream turbines is an attractive solution to provide, with minimal visual impact, predictable and sustainable renewable energy. Whereas tidal energy converters are still in the early stages of development, demonstration arrays of horizontal-axis turbines have been successfully deployed in coastal shelf seas, typically within tidal straits, contributing to the total energy-mix [1]. Successful design and deployment of devices in the marine environment require accurate and refined numerical assessments of the available resource. However, site selection is not simply a question of identifying areas with maximum tidal currents magnitudes, but has to integrate other physical characteristics including consideration of the spatial and temporal variability of the available resource [2]. These aspects are particularly fundamental in locations with strong asymmetry in tidal current magnitude and direction (misalignment) between the flood and ebb phases of the tidal cycle. Numerical simulations of the Orkney archipelago (Scotland, the United-Kingdom) demonstrated that a 30% asymmetry in tidal current velocity may result in a 100% asymmetry in power density [3]. More recently, simulations of the "Raz de Sein" (western Brittany), revealed that pronounced misalignments over 20^{o} (between peak ebb and flood currents) may induce a deficit of over 12% of the monthly averaged extractable energy from a single device. Further effects were expected, at the scale of a tidal turbine array, where interactions between devices may increase the asymmetry in power production between peak ebb and flood [4]. Further, the total energy yield of a given array may be impacted by resource variations over longer time scales experiencing lunar inequalities in relation to differences between (i) spring condition characterized by rated power and (ii) neap condition with sub-optimal power generation [5,6]. Meteorological forcings, and especially wind-generated surface-gravity waves, may also alter tidal currents and modulate the associated power density, with variations exceeding 10% during storm conditions [7–9].

At the stage of turbine farm development, an overall investigation of these variabilities, covering the scale of continental shelf seas, is fundamental in refining site selection. Indeed, besides a local characterization of the available power resource, an advanced comparison between potential tidal stream energy sites will help optimize the geographical distribution of turbines within an array and the aggregation of electricity generation from discrete regions into a unified electricity network [10]. However, refined numerical resource assessments generally focus on a single site, setting aside further comparisons between different locations with strong potential for tidal array development. Apart from local exceptions in western Brittany and the western English Channel [6,11], comparisons between tidal stream energy sites therefore generally rely on large-scale numerical models with spatial resolutions of several kilometers [5,10,12]. Whereas these studies have provided further insights into regional tidal hydrodynamics of interest for potential device developers, the computational grid size remained much larger than the dimension of a turbine, resulting in an approximate definition of tidal characteristics within narrow straits and channels characterized by a complex coastline geometry and significant variations of water depths. With a reduced number of computational grid nodes, large-scale studies are not suitable for resolving the spatial variability of tidal current magnitudes and directions in tidal-stream energy sites with restricted footprints. In the Irish Sea, Lewis et al. [2] reported that regional numerical investigations with a spatial resolution over 1 km may over-estimate the expected power by over 50% from second-generation technologies liable to exploit tidal currents with peak flow over $2\,\mathrm{m\,s^{-1}}$. Stronger uncertainties may result from the approach of current misalignment in these areas, characterized by significant spatial variations of tidal current directions between peak flood and ebb [4,6].

The present investigation complements these large-scale evaluations by exploiting a series of local numerical predictions, at high spatial resolution, in areas of the north-western European shelf seas with strong potential for tidal array development: (i) the Alderney Race in the English Channel, (ii) the Fromveur Strait off western Brittany, (iii) the Pentland Firth and the Firths of the Orkney archipelago in North Scotland (Figs. 1 and 2, Section 2). These locations correspond

naturally to sites with the highest tidal currents magnitudes and associated kinetic energy resource, but also to areas where there has been significant commercial and research interest. Separating the Scottish mainland from the Orkney archipelago, the Pentland Firth is one of the most symbolic illustrations of the tidal energy industry with the MeyGen project (directed by Simec Atlantis Energy) that intends to deploy the world's largest farm of tidal turbines. This project, implemented within the inner sound between the island of Stroma and mainland Scotland (Fig. 3), currently has four 1.5 MW horizontal-axis devices grid connected. With around 70 islands separated by a series of energetic tidal channels, the Orkney archipelago further integrates, as part of the European Marine Energy Centre (EMEC), a full-scale grid-connected tidal test site within the Fall of Warness, the central tidal strait which links the Eastern-north Atlantic to the North Sea through the Firths of Westray and Stronsay [13]. This location is currently experimenting the implementation of a 1 MW tidal-stream turbine as part of the ETI funded ReDAPT project [14]. Another interesting application is the Sabella project (directed by Sabella SAS) that has implemented a 0.5 MW horizontal-axis turbine, off western Brittany, in the Fromveur Strait between the Molène archipelago and the island of Ushant, supplying electricity to the local grid. Various projects are also under consideration to harness the tidal currents of the Alderney Race, considered as one of the most promising locations in the world for large-scale exploitation of the tidal stream energy [15,16]. An advanced comparison of the available tidal stream energy resource with other key locations in north-western European shelf seas will thus help optimize the selection of turbines within these environments.

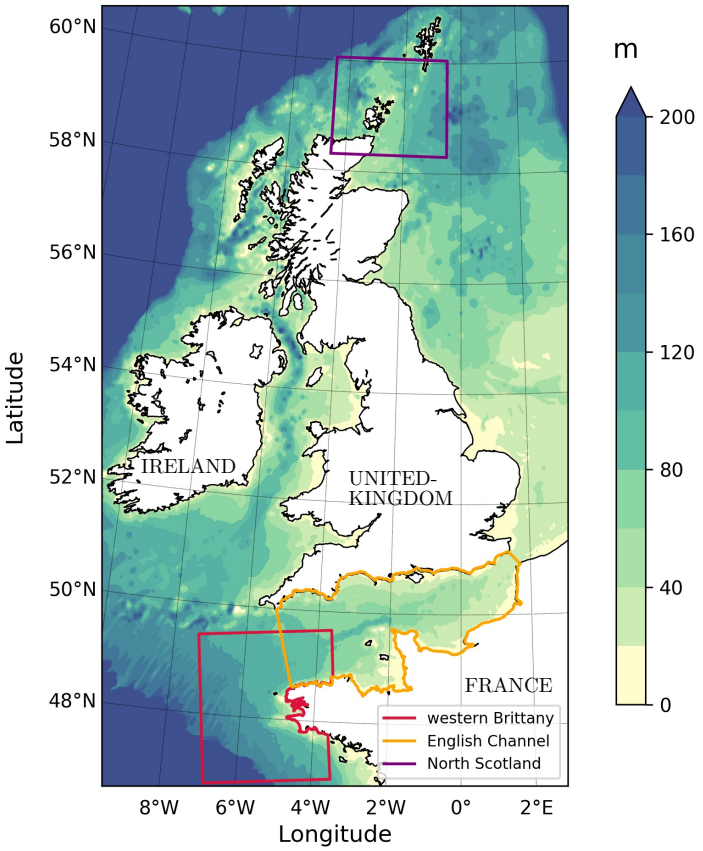

Figure 1. Mean water depths of the north-western European shelf seas with the delimitation of the three computational domains considered in western Brittany, the English Channel and North Scotland.

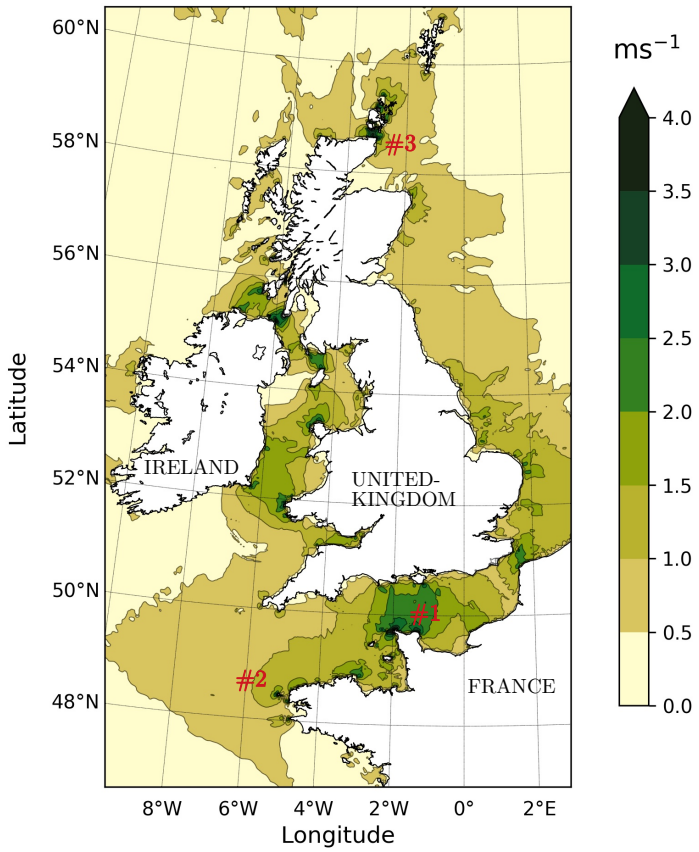

Figure 2. Maximum depth-averaged tidal current magnitudes during a year, recomposed from 10 primary constituents (M_2, S_2, N_2, K_2, K_1, O_1, P_1, Q_1, M_4 and MS_4) across the north-west European shelf seas based on a 2 km tidal harmonic database of depth-averaged current components [6]. The different numbers show the locations of tidal stream energy sites considered in this study: ($\#1$) the Alderney Race, ($\#2$) the Fromveur Strait and ($\#3$) the Pentland Firth and the Firths of Orkney.

Particular attention was first devoted to semi-diurnal asymmetry in tidal current magnitudes between the flood and ebb phases of the tidal cycle, resulting from velocities associated with the principal semi-diurnal lunar component M_2 and its quarter-diurnal harmonic M_4 [17]. The investigation was then conducted on the variability of the available resource between spring and neap conditions from the principal lunar and solar harmonic components M_2 and S_2. Whereas local simulations were based on different models with specific site parameterisations, a consistent approach was adopted across the different computational domains by performing harmonic analysis of predictions of tidal free-surface elevations and depth-averaged currents with the same algorithm developed by Codiga [18] in the `Utide` tidal analysis and prediction package. Following regional resource assessments [5,6], these local harmonic databases were exploited to evaluate the variability of the tidal stream energy resource by calculating a series of metrics based on M_2, S_2 and M_4 harmonics.

After an overall description of the characteristics of tidal stream energy sites including specific information on tidal range, current magnitude and power density (Section 2), particular attention was devoted to the implementation of high-spatial-resolution models (based on depth-averaged and three-dimensional approaches) in the three study areas (western English Channel, western Brittany and North Scotland) (Sections 3-(a) and 3-(b)). We also described the harmonic tidal

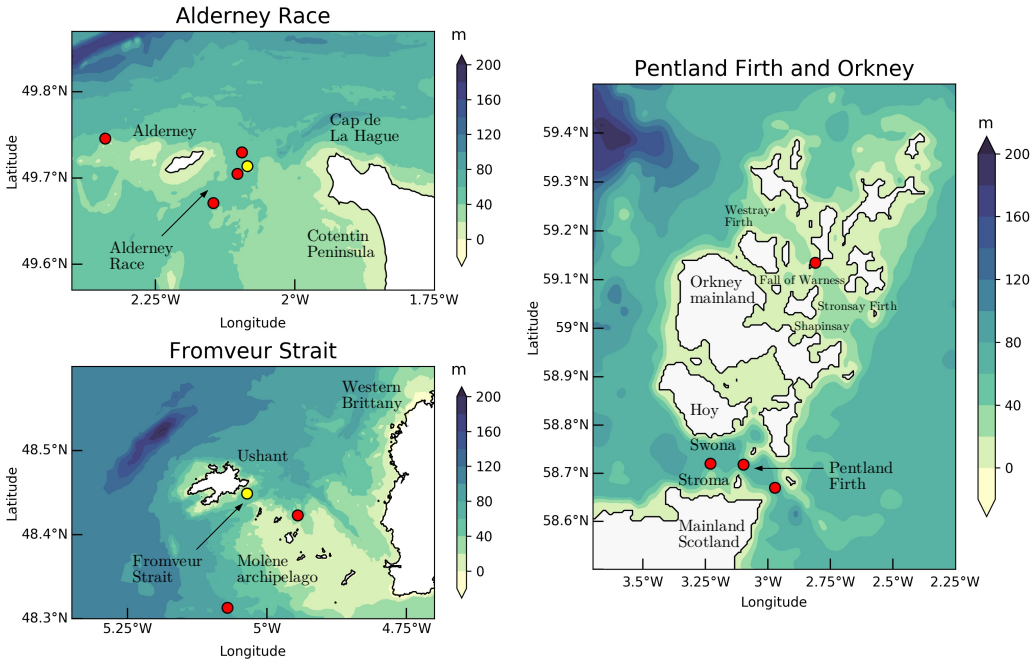

Figure 3. Overview of the bathymetry in the Alderney Race, the Fromveur Strait, the Pentland Firth and the Orkney archipelago. Water depth (in metres) is relative to mean sea level. The locations of current measurements are indicated with red circles. Yellow circles show locations where time series of current observations and measurements were displayed in Figs. 4 and 5.

analysis applied to these local predictions and the tidal energy resource metrics considered to characterise the variabilities in tidal stream power at quarter-diurnal and spring-neap time scales (Section 3-(c)). This investigation resulted in detailed distribution maps of (i) tidal current magnitudes and associated power density (Section 4-(a)) and (ii) tidal current ellipses and energy resource metrics (Sections 4-(b) and 4-(c)). The superimposed effects of wind-generated surface-gravity waves were finally discussed (Section 4-(d)). Beyond a simple assessment based on the highest current magnitudes, these different evaluations provided crucial information identifying areas with (i) near-rectilinear tidal currents favorable for the implementation of fixed-orientation turbines or (ii) with pronounced misalignments more adapted to devices with a yawing mechanism [19]. It also demonstrated the temporal variability of the available resource at semi-diurnal and fortnightly time scales which may be used to characterize the variability in energy extraction, and refine the design of energy converters (e.g., cut-in speed, rated power, etc.). Finally, the potential effects of wind-generated surface-gravity waves may introduce increased temporal variability in the available resource. This information is thus very important to refine the selection of device technology and tidal stream energy sites in north-western Europe (i) demonstrating the attractiveness with respect to resource power variability, and (ii) promoting the development and emergence of the tidal stream sector.

2. Site descriptions

The major characteristics of the different tidal stream stream energy sites are briefly introduced by selecting the Alderney Race as a reference and highlighting differences with the Fromveur Strait, the Pentland Firth and the Firths of Orkney (Westray Firth, Fall of Warness and Stronsay Firth).

This initial site description serves as a basis to highlight and discuss results associated with local high-resolution modelling and associated tidal analysis in computational domains.

Located in the western English Channel, the Alderney Race is a strait with a width of 15 km that separates the island of Alderney (within the Channel Islands) from Cap de La Hague (along the coast of France) (Fig. 3). Water depth is mainly in the range 25 to 45 m with rocky seabed and coarse seabed sediments including pebbles, gravel and rock outcrops [20,21]. The Alderney Race has a mean spring tidal range of over 7 m and mean spring tidal currents that exceed $3.5\,\mathrm{m\,s^{-1}}$ [22]. This tidal stream energy site is characterized by large areas of high current speeds (mean spring currents exceeding $2.5\,\mathrm{m\,s^{-1}}$ over an area of $350\,\mathrm{km^2}$ [6]); hence the interest in large-scale exploitation of the tidal stream energy.

Separating, off western Brittany (France), the island of Ushant from the Molène archipelago, the Fromveur Strait has a width of 2 km (Fig. 3). Mean water depth is approximately 50 m, with increased spatial variations in the vicinity of surrounding islands and islets and rocks of the archipelago. The seabed is highly heterogeneous spatially, typical of tidal strait deposits, with rock and gravel within the strait and localised sand supplies over neighbouring sand banks [23,24]. In spite of a reduced footprint, the Fromveur Strait is recognized as the second largest tidal stream energy site along the coast of France, with a spring tidal range over 7 m, and annual peak velocities exceeding $4\,\mathrm{m\,s^{-1}}$ [25].

Connecting the Atlantic Ocean to the North Sea, the Pentland Firth separates, with a width of 12 km, mainland Scotland from Orkney. This location, with mean water depth of 100 m, is divided into three relatively narrow channels resulting from the presence of the islands of Stroma and Swona: the Inner Sound, the Outer Sound and the South Ronaldsay Channel. Whereas much of the seabed is comprised of rock, areas of mobile sediments exist in the vicinity of headlands and islands, with localised sand supplies such as Sandy Riddle to the east and sandwaves to the west of the island of Stroma [26,27]. In addition to the Pentland Firth, the Orkney archipelago itself incorporates a second channel of interest that extends from the western and eastern approaches of the Fall of Warness (the EMEC tidal test site), including Westray Firth and Stronsay Firth. The mean water depth is between 30 and 50 m in this region, with a seabed resulting from a combination of rocky reefs, exposed bedrocks and sedimentary substrates [28,29]. The Orkney archipelago and the Pentland Firth act furthermore as a significant sink of tidal energy resulting in a reduced mean spring tidal range between 3 and 4 m, typical of mesotidal conditions [30,31]. Numerical simulations estimated that peak spring tidal currents were reaching a magnitude of $5\,\mathrm{m\,s^{-1}}$ in the Pentland Firth with values of $3.7\,\mathrm{m\,s^{-1}}$ in the Fall of Warness [3,26].

3. Materials and methods

The present study was based on the exploitation (from tidal harmonic analysis) of a series of refined numerical resource assessments to investigate different properties associated with the exploitation of the tidal stream energy resource (including current misalignment and resource variability at semi-diurnal and fortnightly time scales). Whereas differences may appear with respect to the numerical approach (numerical resolution, grid spacing, time steps, etc.), calibration (e.g. bed roughness) and sources of data (e.g. bathymetry and boundary conditions) [24,32], predictions were assessed against available observations of tidal range and currents. We assumed here that the existing validations were sufficient to conduct a comparison of numerical predictions in the three tidal stream energy sites. A series of site-specific research studies was furthermore conducted on the basis of these simulations which provided further references to analyse and discuss the results obtained from harmonic analysis of numerical predictions.

(a) Model setup

Simulations within the Alderney Race and the Fromveur Strait were conducted with the two-dimensional (2D) horizontal model Telemac 2D [33]. The model resolves the shallow water Barré de Saint-Venant equations of continuity and momentum on a planar unstructured computational

grid, particularly suited to capturing the complex shoreline topography and spatial variations in water-depth at tidal stream energy sites. Predictions within the Alderney Race were derived from the implementation of Thiébot et al. [34] with a computational domain that extended over the English Channel to achieve suitable open boundary conditions (Fig. 1). The computational grid was composed of 66,494 nodes with a spatial resolution of around 5 km at offshore sea boundaries to 200 m within the Race. Predictions within the Fromveur Strait relied on the implementation performed by Guillou and Chapalain [35,36] with 51,226 nodes and a spatial resolution varying from 10 km offshore to 50 m within the Strait. In both cases, assuming logarithmic vertical velocity profiles, a quadratic bottom friction law was adopted and formulated with respect to the bottom roughness z_0. Following Guillou and Thiébot [24], z_0 was parameterised in terms of physical roughness of the bed with respect to the different sediment bottom types identified by Vaslet et al. [37] in the western English Channel and by Hamdi et al. [38] in western Brittany. In these two implementations of Telemac 2D, the horizontal momentum diffusion coefficient (eddy viscosity) was computed with a depth-averaged $k-\varepsilon$ model. Neglecting the influences of atmospheric pressure, wind velocity components and surface-gravity waves, both models were driven by sea level variations and depth-averaged velocities recomposed from harmonic tidal constituents of the TPXO8-atlas database [39].

Simulations in the Pentland Firth and within the Orkney archipelago were derived from the implementation by Neill et al. [3] of the three-dimensional ROMS model (Regional Ocean Modelling System) based on the Reynold-Averaged Navier Stokes equations [40]. The computational domain extended to the North, encompassing part of Shetland at a horizontal grid spacing of around 500 m (Fig. 1). Simulations were parameterised with a uniform quadratic drag friction coefficient set up at $C_D = 0.003$, while turbulent parameters derived from the Generic Length Scale formulation were tuned to represent the $k-\varepsilon$ model [41]. The model was driven at the sea boundaries by FES2012 currents and elevations for the principal harmonic constituents [42].

(b) Model validation

Simulations within the Alderney Race were compared with ADCP observations acquired by OpenHydro at five locations around the island of Alderney [21]. An overall good agreement was, in particular, obtained for the current magnitude in the center of the Race, with a root-mean-square-error (RMSE) of $0.24\,\mathrm{m\,s^{-1}}$ over the period of the observations (between 12 July and 17 August 2014) (Fig. 4). Predictions also reproduced the abrupt changes of current direction between the northeast and southwest directions.

In the Ushant-Molène archipelago, model performance in assessing tide-induced vertical variations was confirmed by a comparison of the predicted and observed M_2 component at a tide gauge in the harbor of Ushant (predicted magnitude of 2.07 m versus observed value of 2.09 m and predicted phase of 111.0^{o} relative to Greenwich versus an observed value of 99.9^{o}) [43]. This local assessment was complemented by a comparison with in-situ ADCP current observations, acquired by the French Navy SHOM ("Service Hydrographique et Océanographique de la Marine"), at three locations in and around the Fromveur Strait [24,36,43]. The model reproduced, in particular, the magnitudes of tidal currents within the Strait with a normalized RMSE of 14.1% over the period of the observations (between 20 March and 2 April 1993) [36] (Fig. 5).

In the Pentland Firth and the Orkney archipelago, the numerical model was first validated by comparing predicted amplitudes and phases of M_2 and S_2 harmonic components with observations at a series of 14 tidal gauge stations published in the Admiralty Tide Tables [3]. The averaged RMSE from a 15 days simulation was estimated at 8.3 cm and 3.7 cm for the amplitudes of M_2 and S_2, respectively. The associated RMSE for tidal phases of M_2 and S_2 was 6.8 and 7.5^{o}, respectively. This evaluation was complemented by a detailed analysis of tidal current constituents based on an available 32 day ADCP mooring at the Fall of Warness. This local assessment showed differences restricted to less than 3% for the evaluation of M_2 current magnitude. This configuration of ROMS was furthermore assessed by Goward-Brown et al. [44]

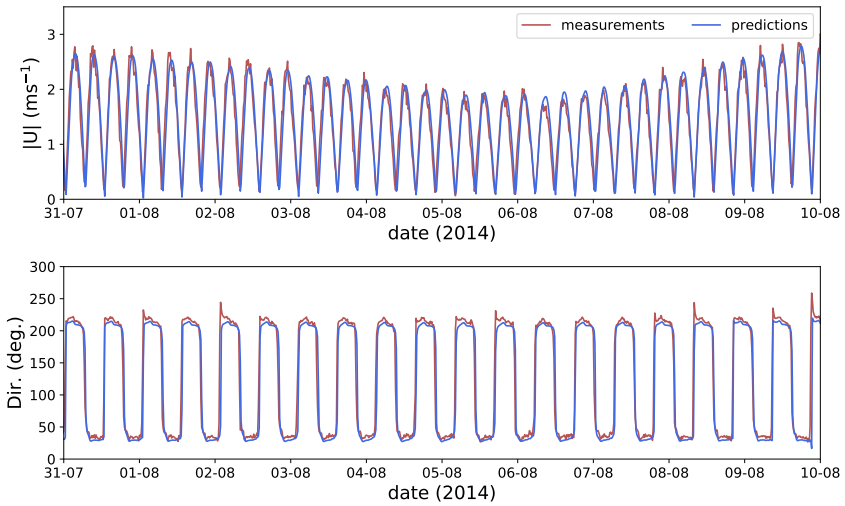

Figure 4. Observed and simulated time series of the magnitude and direction (anticlockwise convention from the east) of the depth-averaged current within the Alderney Race (longitude $= 2.085^{o}$ W;latitude $= 49.714^{o}$ N).

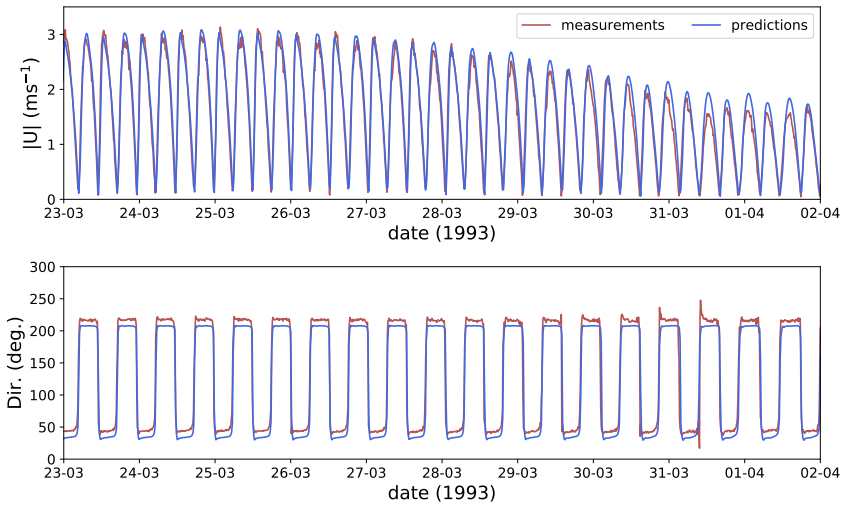

Figure 5. Observed and simulated time series of the magnitude and direction (anticlockwise convention from the east) of the current 10 m above the bed within the Fromveur Strait (longitude $= 5.036^{o}$ W;latitude $= 48.449^{o}$ N).

in the Pentland Firth by exploiting ADCP current measurements, deployed at three locations by Guardline Surveys on behalf of the Navigation Safety Branch of the Maritime and Coastguard Agency. In spite of a reduced variability, predictions reproduced the observed magnitudes and directions of depth-averaged currents. The total RMSE for the amplitudes and phases of tidal current velocity for the principal M_2 and S_2 components were estimated at $0.21\,\mathrm{m\,s^{-1}}$, $0.04\,\mathrm{m\,s^{-1}}$, and 5^{o} and 13^{o}, respectively.

(c) Application of numerical predictions

For the consistent application of the numerical predictions to understand tidal energy, simulations were driven by the principal lunar M_2 and solar S_2 harmonic components, and the first quarter-diurnal harmonic M_4. Tidal analysis was performed on simulated surface elevations and depth-averaged velocities to produce a harmonic database for these three components. This treatment was performed by relying on the implementation in Python of the `Utide` tidal analysis and prediction package originally developed in Matlab by Codiga [18]. An ordinary least squares method was adopted. The resulting tidal harmonic database was used to produce a series of tidal energy resource metrics, characterizing the spatial and temporal variabilities of tidal current magnitudes and associated stream power.

At the quarter-diurnal time scale, current asymmetry was characterised, following Guillou et al. [6], by the ratio

$$\mathrm{Var}_{asym} = \frac{\overline{u}_{max}(\mathrm{M}_4)}{\overline{u}_{max}(\mathrm{M}_2)} |\cos\gamma| \tag{3.1}$$

between the maximum magnitudes of depth-averaged currents resulting from M_2 and M_4, $\overline{u}_{max}(\mathrm{M}_2)$ and $\overline{u}_{max}(\mathrm{M}_4)$. $\gamma = 2\phi(\mathrm{M}_2) - \phi(\mathrm{M}_4)$ accounts for the phase shift between these two harmonic components, with $\phi(\mathrm{M}_2)$ and $\phi(\mathrm{M}_4)$ the associated phases (degrees relative to Greenwich). Indeed, as exhibited by Pingree and Griffiths [45] and Friedrichs and Aubrey [46], the asymmetry of tidal current magnitudes between peak ebb and flood may arise from the phase relationship γ with (i) maximum asymmetry when M_2 and M_4 are in phase ($\gamma = 0^o$ or 180^o) and (ii) minimum asymmetry when both components are out of phase ($\gamma = 90^o$ or 270^o). High values of Var_{asym} therefore indicate increased tidal asymmetry, whilst low values indicate more symmetrical currents magnitudes and reduced intermittency between peak ebb and flood.

At the spring-neap time scale, tidal variability was assessed, following Robins et al. [5] and Guillou et al. [6], by the ratio

$$\mathrm{Var}_{sn} = 1 - \frac{\overline{u}_{max}(\mathrm{S}_2)}{\overline{u}_{max}(\mathrm{M}_2)} \tag{3.2}$$

between the maximum magnitudes of depth-averaged currents resulting from M_2 and S_2, $u_{max}(\mathrm{M}_2)$ and $u_{max}(\mathrm{S}_2)$. As the magnitude of S_2 remains weaker than M_2 over the northwest European shelf seas, and indeed most semidiurnal regions of the world, this ratio varies between 0 and 1. Reduced values of Var_{sn} (close to 0) account for increased differences between spring and neap tidal conditions, whilst high values (close to 1) show reduced temporal variability, more attractive conditions for the implementation of tidal kinetic energy converters.

Finally, tidal ellipses were investigated by relying on predictions of eastward and northward velocity components during a tidal cycle. The rectilinear or circular nature of tidal currents was assessed with the ellipticity defined, for a single harmonic component, as the ratio between magnitudes of the semi-minor $\overline{u}_{min}$ and semi-major $\overline{u}_{max}$ axes of the tidal current ellipse $r = \overline{u}_{min}/\overline{u}_{max}$. Further details about the mathematical formulations of minimim and maximum magnitudes $\overline{u}_{min}$ and $\overline{u}_{max}$, and phases ϕ are available in [47] and [6].

4. Results and discussion

(a) Tidal range, current magnitude and power density

Before investigating the temporal variability of the available resource, integrated parameters obtained from the tidal analysis of the numerical predictions were first considered. This includes the magnitudes and phases of principal harmonic components for the free-surface elevations, the peak magnitudes of recomposed depth-averaged currents, and the associated power density. Co-tidal charts of the principal semi-diurnal lunar component M_2 in the three computational domains show considerable variations in tidal range between sites located (i) along the coast of France and (ii) in North Scotland (Fig. 6). Confirming previous numerical investigations in these areas [3,43,48], the amplitude of the M_2 component in the Fromveur Strait and the Alderney Race

is around twice the value predicted in the Orkney archipelago. The result of the tidal analysis in the Orkney archipelago corroborated furthermore the noticeable time lag of semi-diurnal tidal waves between the North Atlantic Ocean and the North Sea. For the principal M_2 component, this time lag was estimated between 50 and 60^o (around 2 hours) between both approaches to the Pentland Firth and channels in the Orkney archipelago. This phase lag was, however, reduced to under 5^o in the Fromveur Strait and the Alderney Race, with nearly equal times for high and low tides. A clear contrast was thus exhibited between tidal stream energy sites (i) in western Brittany and the western English Channel (with increased tidal ranges and reduced phase lags) and (ii) in North Scotland (with reduced tidal ranges and increased phase lags). This suggested different spatial and temporal evolutions of tidal currents.

The spatial distribution of the peak tidal current magnitudes resulting from M_2, S_2 and M_4 highlights the potential of the three areas for tidal stream energy exploitation (Fig. 7). Confirming previous studies [3,21,24,31], predicted maximum magnitudes ranged from $4.1\,\mathrm{m\,s^{-1}}$ within the Fromveur Strait to $5.1\,\mathrm{m\,s^{-1}}$ within the Pentland Firth. The increased value in North Scotland resulted mainly from a strong hydraulic gradient across tidal channels associated with the increased phase lag in tidal free-surface elevation [26]. We retained the criteria adopted by a series of numerical investigations around the United-Kingdom to identify potential locations for first- and second-generation technologies of tidal stream energy converters, matching both devices currently tested in the marine environment or at the early stages of development [2,5,49]. This corresponds to areas with water depths that exceed 25 m and mean spring tidal current magnitudes over 2.5 and $2.0\,\mathrm{m\,s^{-1}}$, respectively. A clear contrast was exhibited between (i) the Alderney Race and the Pentland Firth that showed large areas of high current magnitudes and (ii) the Fromveur Strait and the Fall of Warness with reduced footprints (Tab. 1). The sea space for tidal stream energy exploitation increased markedly for second generation technologies confirming the interest in developing turbines capable of harnessing less energetic tidal streams [6,12]. However, reduced areas were obtained by applying the criteria adopted by the Carbon Trust [50] – identifying locations where the power density, averaged over a spring-neap tidal cycle, exceeded the rated value of $2.5\,\mathrm{kW\,m^{-2}}$ (Fig. 8 and Tab. 1). The estimate of $76\ \mathrm{km^2}$ within the Alderney Race is consistent with the value of $93\ \mathrm{km^2}$ obtained by Coles et al. [11] based on the recomposition of tidal current time series with nine major harmonic components instead of three (M_2, S_2 and M_4 in the present investigation). This second criteria resulted in greater areas suitable for turbines within the Pentland Firth than within the Alderney Race ($110\ \mathrm{km^2}$ against $76\ \mathrm{km^2}$), whereas the opposite situation was obtained with the first criteria (based on tidal current magnitude) ($135\ \mathrm{km^2}$ in the Pentland Firth against $162\ \mathrm{km^2}$ in the Alderney Race, Tab. 1). Indeed, the Alderney Race was characterized by a concentration of mean kinetic power density around the Cotentin Peninsula, where values locally exceeded $7\,\mathrm{kW\,m^{-2}}$ but restricted below $5\,\mathrm{kW\,m^{-2}}$ elsewhere, whereas the Pentland Firth exhibited large areas of high energy in the vicinity of islands (including Stroma, Swona, Muckle Skerry and the Pentland Skerries on its eastern side) (Fig. 8) [31,51].

These differences also highlighted the uncertainties in relying on integrated parameters to characterize the available resource at tidal stream energy sites. We tested the relevance of using the peak current magnitude in mean spring conditions (which is a local temporal indicator) by comparing it to the available power density averaged over a spring-neap tidal cycle (which integrated the temporal variations of the current magnitude) (Fig. 9). Different correlations were obtained in the Alderney Race and the Pentland Firth. Locations with $\overline{u}^{max}_{spring}$ between 3.5 and $4\,\mathrm{m\,s^{-1}}$ revealed a linear trend in the evolution of $P^{mean}_{neap-spring}$ within the Alderney Race, whereas increased dispersion was obtained between these two variables ($\overline{u}^{max}_{spring}$ and $P^{mean}_{neap-spring}$) within the Pentland Firth. Refined investigations of temporal variability of the available resource were thus required.

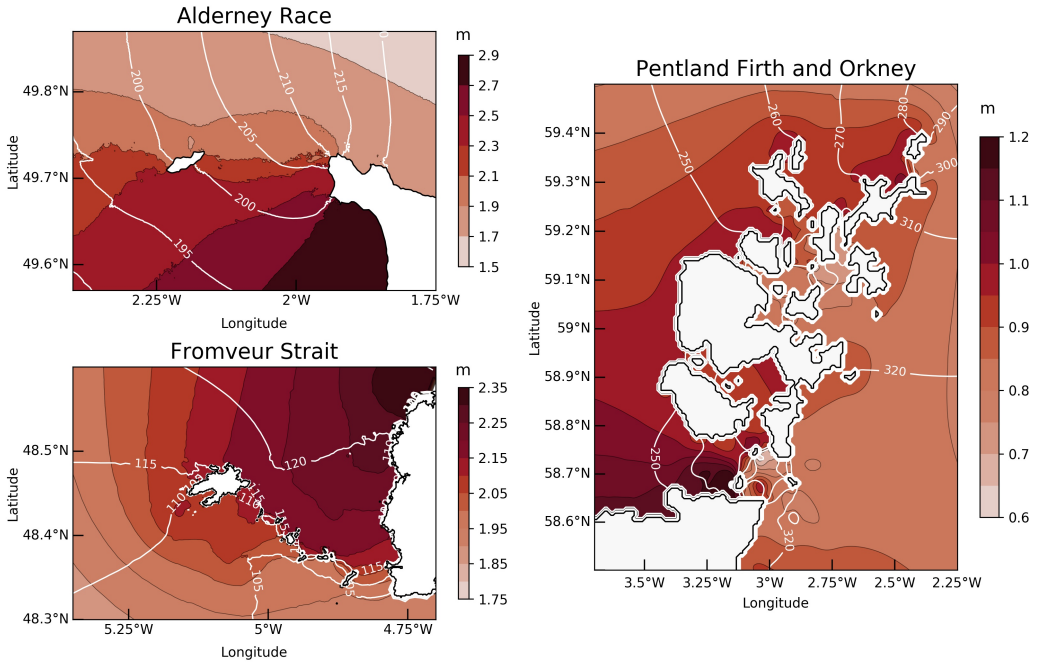

Figure 6. M_2 co-tidal charts in the Alderney Race, the Fromveur Strait and the Pentland Firth and Orkney archipelago.

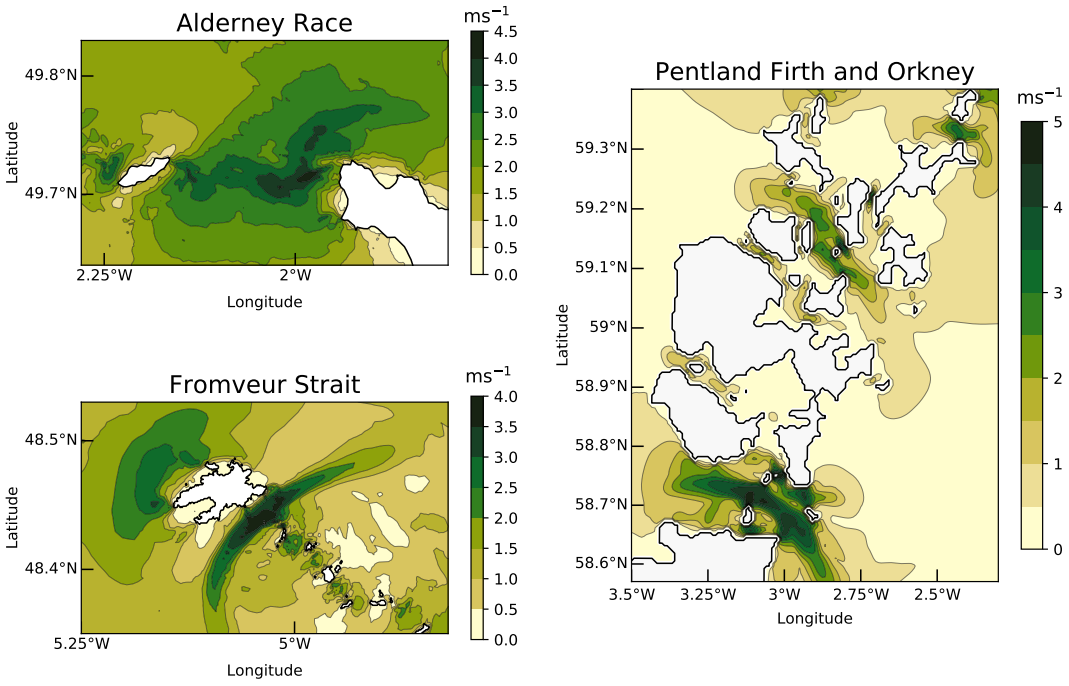

Figure 7. Peak magnitudes of depth-averaged tidal currents, $\overline{u}^{max}_{spring}$, resulting from M_2, S_2 and M_4 harmonic components.

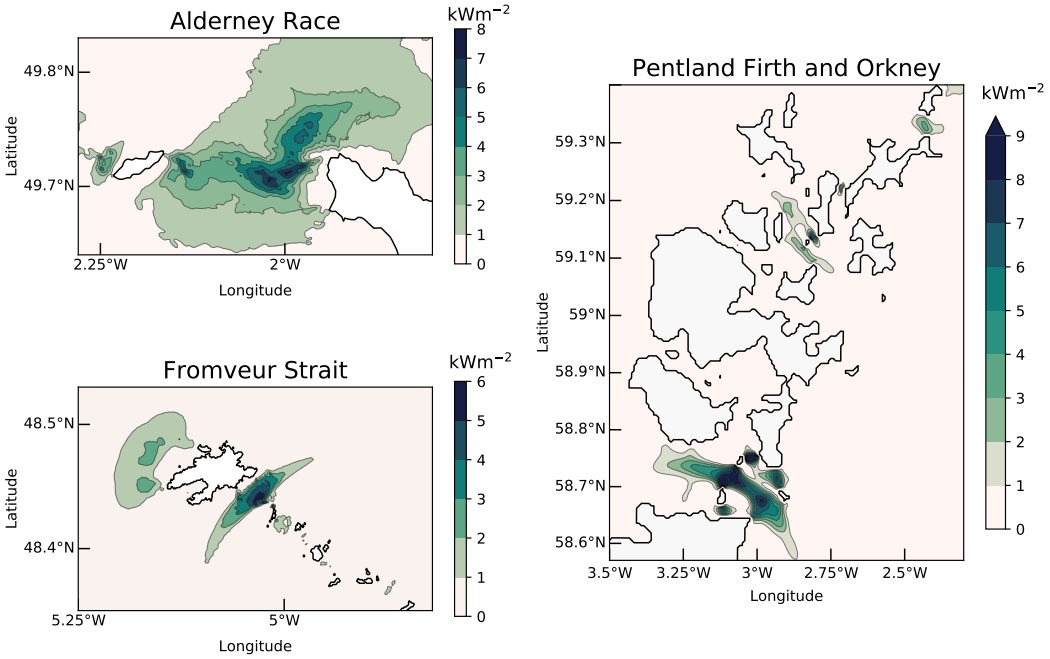

Figure 8. Distribution of averaged kinetic power density during a spring-neap tidal cycle (T=14.765 days), $P^{mean}_{neap-spring}$, based on M_2, S_2 and M_4 harmonic components.

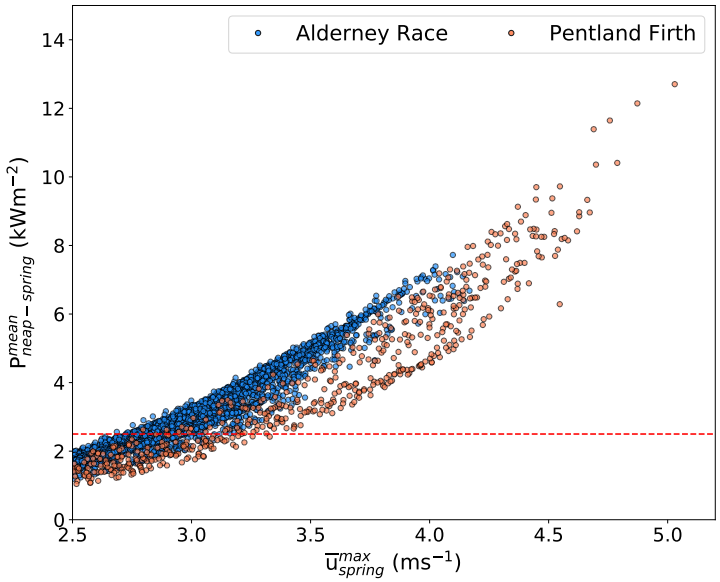

Figure 9. Peak magnitudes of depth-averaged tidal currents resulting from M_2, S_2 and M_4 harmonic components against averaged associated power density during a neap-spring tidal cycle within the Alderney Race and the Pentland Firth. The horizontal red dotted line refers to the value of 2.5 kW m^{-2} for the power density.

Table 1. Extents of areas where peak spring currents (based on M_2, S_2 and M_4) exceed $2.5\,\mathrm{m\,s^{-1}}$ and $2.0\,\mathrm{m\,s^{-1}}$, the rated values for first and second-generation turbines respectively, with mean water depths over 25 m within the Alderney Race, the Fromveur Strait, the Pentland Firth, and the Firths of Orkney. Areal extents where the power density, averaged over a spring-neap tidal cycle, exceeds $2.5\,\mathrm{kW\,m^{-2}}$ in these tidal stream energy sites.

Tidal stream energy site	Areal extent ($\mathrm{km^2}$) $\overline{u}^{max}_{spring} > 2.5\,\mathrm{m\,s^{-1}}$	$\overline{u}^{max}_{spring} > 2.0\,\mathrm{m\,s^{-1}}$	$P^{mean}_{neap-spring} > 2.5\,\mathrm{kW\,m^{-2}}$
Alderney Race	162	>418	76
Fromveur Strait	16	25	7
Pentland Firth	135	197	110
Firths of Orkney	10	27	5

(b) Tidal current asymmetry

Tidal ellipses for the principal semi-diurnal lunar component M_2 confirmed that near-rectilinear flows prevailed at tidal stream energy sites (Fig. 10). However, the western part of the Pentland Firth was characterized by increased ellipticity, seemingly associated with the complex circulations in the vicinity of headlands and islands. In this region, confirming previous numerical investigations [44], the residual currents from M_2 and M_4 components revealed important recirculations extending over the width of the tidal channel (Fig. 11). The near-rectilinear nature of tidal currents represents favourable conditions for the installation of fixed-orientation turbines, matching the majority of technologies currently implemented in the marine environment. The temporal variability of the available resource can thus be characterized by assessing the variations of tidal current magnitudes between peak ebb and flood (from parameter Var_{asym}) and between spring and mean conditions (from parameter Var_{sn}), setting aside variations in current directions at tidal stream energy sites.

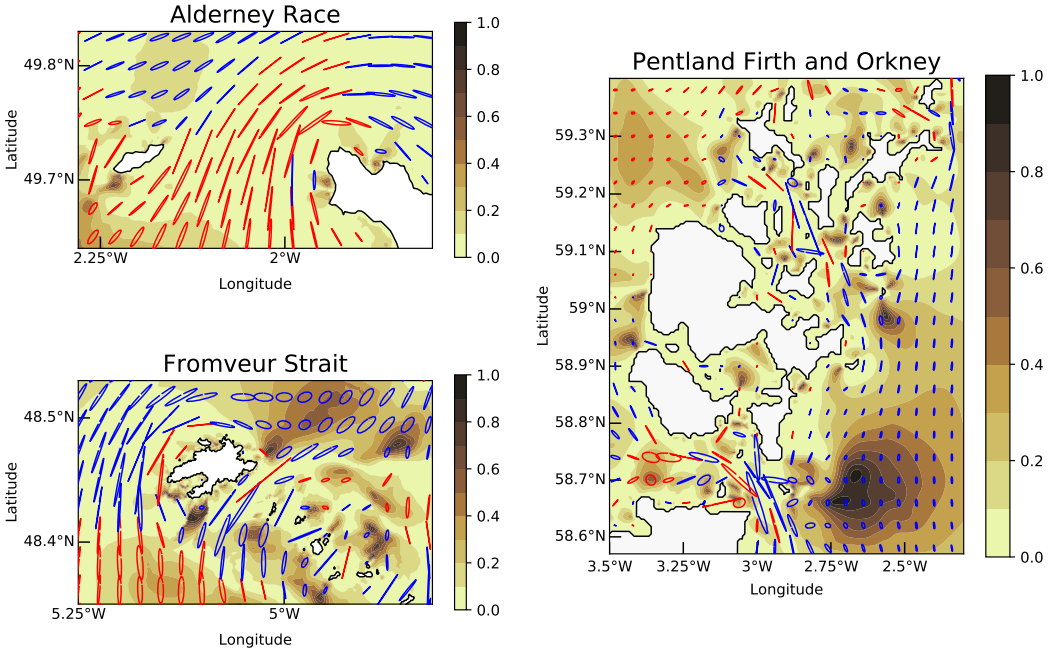

Figure 10. M_2 tidal current ellipses with ellipticity shown as colorscale. Blue and red ellipses indicate clockwise and anti-clockwise rotations, respectively.

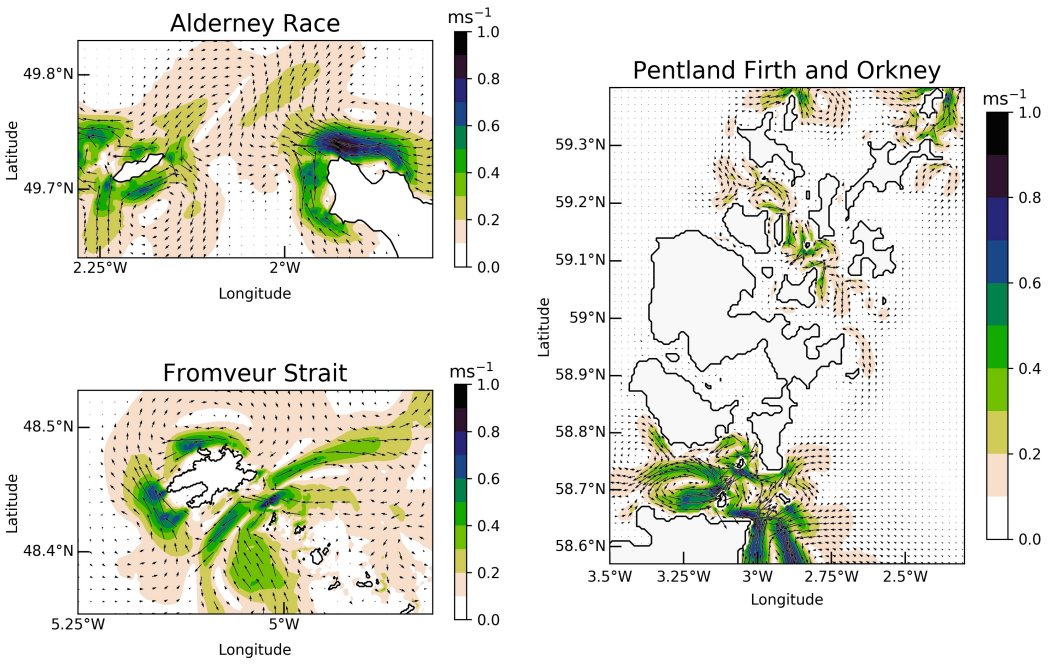

Figure 11. Residual depth-averaged tidal currents resulting from M_2 and M_4 harmonic components over an M_2 tidal cycle.

A strong correlation was obtained in energetic areas of the Fromveur Strait between magnitudes of (i) Var_{asym} (which characterizes the variability of the resource between peak ebb and flood), and (ii) the residual depth-averaged tidal currents resulting from M_2 and M_4 (Fig. 12). The spatial distribution of these two parameters in the three computational domains revealed similar patterns, confirming regional investigations conducted across the north-western European shelf seas and along the coast of France [5,6] (Figs. 11 and 13). Tidal stream energy sites exhibited different semi-diurnal asymmetries that were reduced in the Alderney Race and more pronounced in the Fromveur Strait and in North Scotland. In the Alderney Race, differences were mainly exacerbated towards the edges of the tidal channel, in the vicinity of the island of Alderney and Cap de La Hague, revealing a very important region with reduced asymmetry in tidal current magnitude, making this a desirable region for tidal energy conversion. In accordance with local investigations [43,52], the Fromveur Strait exhibited significant asymmetry in a north-eastern region, experiencing flood-dominated flows, and a south-western region with ebb-dominated flows. A central divergence zone had reduced differences in the technically exploitable power at peak ebb and flood. In spite of a complex residual circulation marked by a series of eddies around islands and headlands, the Pentland Firth and Orkney waters revealed important exploitable areas. Extended areas with reduced asymmetries appeared thus (i) in the eastern part of the Pentland Firth from the islands of Stroma and Swona to Muckle Skerry, and (ii) within Westray Firth, in the the north-western part of Orkney. In the Pentland Firth, these results appeared consistent with ADCP observations of current magnitudes conducted for the Navigation Safety Branch of the Maritime and Coastguard Agency (Fig. 3). The location in the western part of the Pentland Firth was characterised by increased asymmetry ($\text{Var}_{asym} = 0.143$) with differences exceeding $0.5\,\text{m}\,\text{s}^{-1}$ between peak ebb and flood [30], while reduced asymmetry was found between Stroma and Swona ($\text{Var}_{asym} = 0.008$) and in the eastern part of the tidal channel ($\text{Var}_{asym} = 0.011$). In the major Firths of Orkney, our results also confirmed the analysis

conducted by Neill et al. [3] with more pronounced asymmetry in the south-eastern part of the tidal channel than in its north-western part.

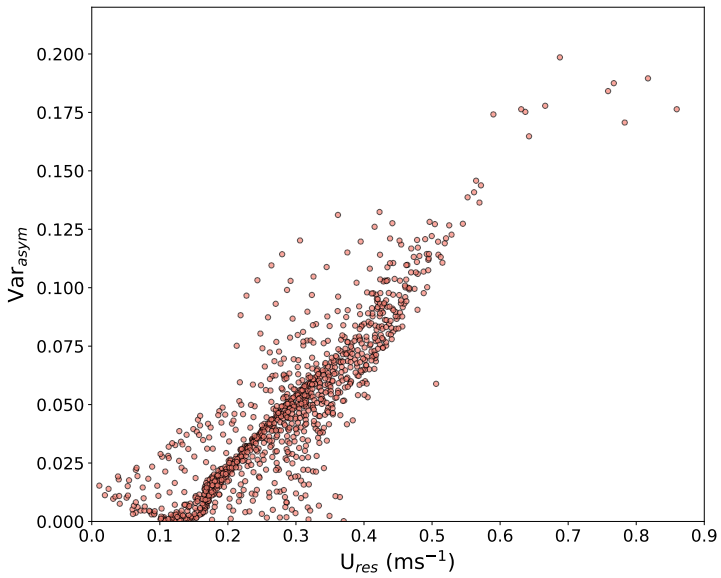

Figure 12. Residual depth-averaged tidal currents resulting from M_2 and M_4 against parameter Var_{asym} for areas with ellipticity below 0.04 (strongly rectilinear) and $\overline{u}_{max}(M_2) > 2.0\,\mathrm{m\,s^{-1}}$ within the Fromveur Strait.

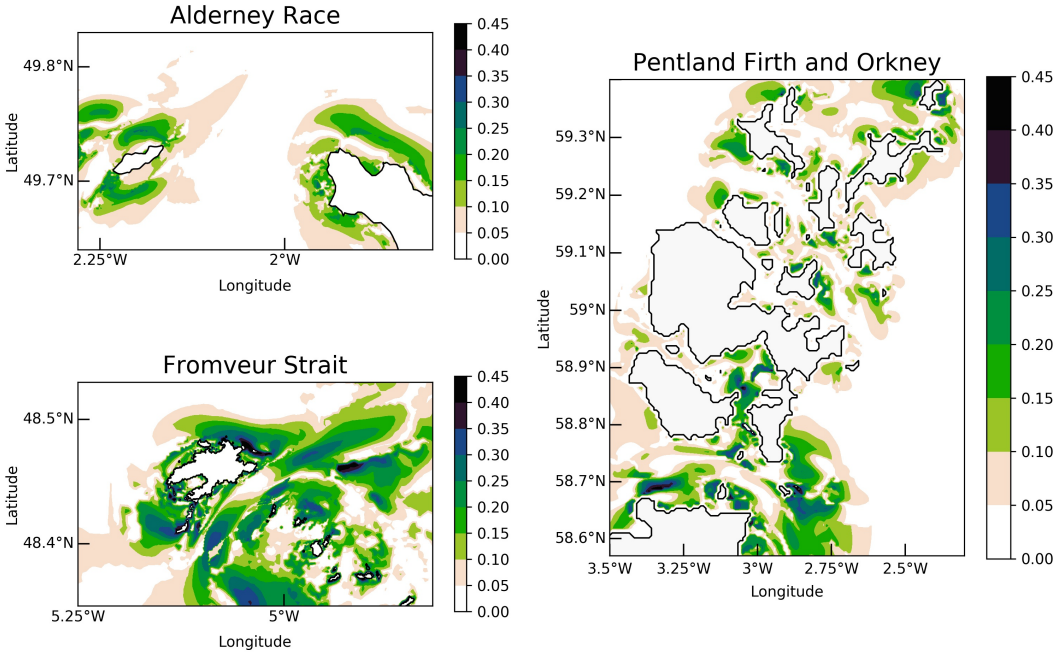

Figure 13. Spatial distribution of parameter $Var_{asym} = \overline{u}_{max}(M_4)/\overline{u}_{max}(M_2)|cos(\gamma)|$ with $\gamma = 2\phi(M_2) - \phi(M_4)$.

(c) Spring-neap variability

In agreement with the regional numerical investigations conducted in the north-western European shelf seas [5] and along the coast of France [6], there was a clear contrast in spring-neap tidal variability of current magnitudes between (i) the Alderney Race characterized by reduced variability ($\mathrm{Var}_{sn} > 0.67$) and (ii) the Ushant-Molène archipelago with increased variability ($\mathrm{Var}_{sn} < 0.62$) (Fig. 14). Simulations at high-spatial resolution provided, however, an increased definition of spring-neap tidal variability at the scale of tidal stream energy sites. In western Brittany, the area surrounding the Molène archipelago and including the Fromveur Strait had thus reduced variability, leading to more attractive energy conversion. Nevertheless, the area of North Scotland exhibited more significant spring-neap tidal variability ($\mathrm{Var}_{sn} < 0.62$). The difference was particularly noticeable between the Pentland Firth ($\mathrm{Var}_{sn} < 0.62$) and the Alderney Race ($\mathrm{Var}_{sn} > 0.67$). In spite of smaller values obtained here and seemingly associated with different spatial resolutions, such difference was also reported by Robins et al. [5] highlighting less spring-neap variability of the available resource in the Alderney Race than in the Pentland Firth. Robins et al. [5] therefore estimated that, for locations with equivalent mean spring peak tidal current magnitudes, there was a reduction of around 10% in the annual technical power generated by a Seagen-S 1.2 MW rated turbine between the Pentland Firth ($\mathrm{Var}_{sn} = 0.69$) and the Alderney Race ($\mathrm{Var}_{sn} = 0.75$). As peak spring currents exceeded the rated speeds of turbines, differences in the technically exploitable power over lunar timescales were mainly associated with differences that occurred during neap tides. The Alderney Race was therefore characterized by increased magnitudes of neap tidal currents, resulting in increased technical power. During neap tides, Guillou et al. [6] showed a reduction of around 30% of the maximum power, generated by a 1.5 MW rated turbine, between a site in the Alderney Race ($\mathrm{Var}_{sn} = 0.69$) and a site in the Fromveur Strait ($\mathrm{Var}_{sn} = 0.63$). The averaged generated power showed, however, reduced differences, whereas strong variability may occur between spring and neap tides.

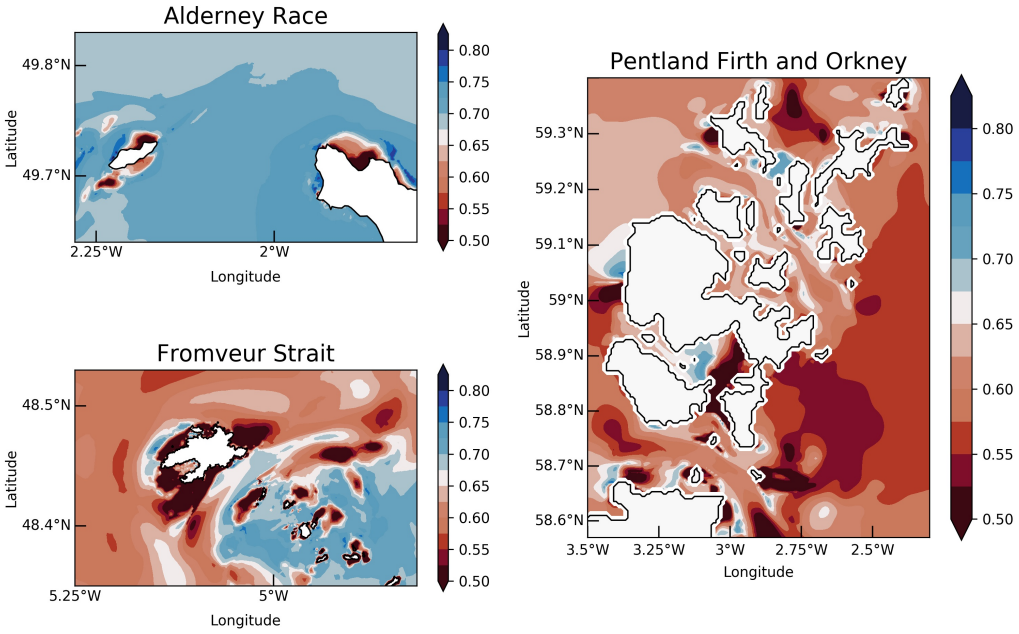

Figure 14. Spatial distribution of $\mathrm{Var}_{sn} = 1 - \overline{u}_{max}(\mathrm{S}_2)/\overline{u}_{max}(\mathrm{M}_2)$.

(d) Superimposed effect of waves

So far, we have focused on temporal variability of the tidal stream power resource neglecting the influence of additional processes such as meteorological forcings (e.g., winds) and wind-generated surface-gravity waves. Besides the effects that wind may have on near-surface currents, waves may also influence tidal currents and associated kinetic energy through two non-linear processes, by (i) increasing the apparent bottom friction felt by currents above the wave boundary layer, and (ii) generating wave-induced currents [53,54]. These effects may be important in tidal stream energy sites of north-western European shelf seas, characterized by energetic waves climates with significant wave height liable to exceed 4 m (Fig. 15). These effects were, in particular, investigated in western Brittany by coupling wave and tidal circulation models during storm conditions [9]. Whereas the Fromveur Strait was protected from North-Atlantic incoming waves by the isle of Ushant, waves were subjected to significant depth- and current-induced refraction entering the southern part of the tidal channel, leading to important wave and current interactions with conditions of waves opposing currents [56]. Predictions show a reduction of the available mean spring tidal power density by around 12% during storm conditions (characterized by offshore significant wave height over 5 m and peak period exceeding 14 s). Strong wave and current interactions have also been documented in the Pentland Firth [57]. Indeed, this tidal stream energy site was characterized by a direct exposure to North-Atlantic westerly incoming waves that were almost aligned with tidal currents [31]. This resulted in significant wave and current interactions manifested as tidal modulations in the significant wave height [57,58]. Whereas the western English Channel experienced important wave energy dissipation by bottom friction, the Alderney Race may be also subjected to significant energetic events, with significant wave height liable to exceed 6 m [59]. In spite of increased spreading of the incoming wave direction, there were clearly important angles between wave and current directions that were liable to minimize the effects waves may have on the currents in this tidal stream energy site. However, Bennis et al. [60] recently demonstrated that waves may significantly alter the vertical distribution of the current velocity magnitude in this environment.

The north-western European tidal stream energy sites considered here therefore had strong wave and current interactions liable to impact the tide-induced variability of the kinetic energy of tidal currents. However, these effects were mainly exhibited for stationary offshore wave conditions, setting aside the temporal variability of the wave energy flux over continental shelf seas [8,9]. Over the north-west European shelf seas, waves are characterized by strong seasonal and inter-annual variations globally characterized by (i) low and nearly stable wave power during spring and summer, and (ii) energetic and time-varying energy flux during autumn and winter [55,61]. During the winter period, the most energetic month may vary between December

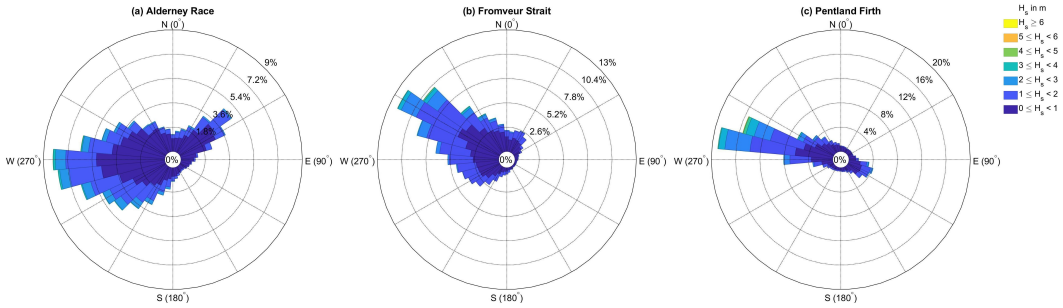

Figure 15. Wave roses computed over a ten year period (2003-2012) based on regional simulations conducted by Neill et al. [55].

and March [62]. The temporal variability of the wave energy flux may thus influence the tide-induced variability of the available resource at the four sites considered in the present study. Additional temporal variabilities may be expected when considering the modulation induced by tidal currents on (i) the interaction between wave and current bottom boundary layers and (ii) the wave propagation. Further numerical investigations are thus required regarding the effects of non-stationary waves and current interactions on the available tidal stream energy resource.

5. Conclusion

In this review, we exploited high-resolution numerical simulations of the tide-induced circulation to compare and investigate the temporal variability of the available resource in different stream energy sites across the north-western European shelf seas: the Alderney Race in the western English Channel, the Fromveur Strait off western Brittany, the Pentland Firth and the Firths of the Orkney archipelago in North Scotland. Tidal analysis was performed on model predictions to derive the spatial distribution of the magnitudes and phases of major harmonic components M_2 and S_2, and quarter-diurnal harmonic M_4 for tidal water elevations and depth-averaged currents. This constituent data was exploited to produce detailed cartographies of time-integrated parameters such as the maximum tidal current magnitude and mean available power density. We also computed a series of tidal energy resource metrics based on harmonic components to characterize the current asymmetry (based on M_2 and M_4) and spring-neap tidal variability (based on M_2 and S_2). The main outcomes of the present study are as follows:

(i) The Alderney Race and the Pentland Firth contain large areas (> 130 km^2) of high current speed (peak spring current > 2.5 m s^{-1}) that appeared suitable for the implementation of first-generation tidal turbines. This total exploitable area was around one tenth of this size in the Fromveur Strait and the Orkney channel (Fall of Warness).

(ii) Tidal stream energy sites were characterized by significant spatial variability in the magnitude of the available power density. This distribution was particularly noticeable in the Alderney Race, with a concentration of the averaged power density (during a spring-neap tidal cycle) exceeding 6 kW m^{-2} near Cap de La Hague.

(iii) Rectilinear tidal currents prevailed at stream energy sites, suitable for the installation of fixed-orientation devices. But this property of tidal currents also confirmed that the temporal variability of the available resource (between peak ebb and flood or between spring and neap conditions) may be investigated by relying on the magnitudes of harmonic components, regardless of the effects of current directions.

(iv) There was a clear contrast between the Alderney Race (with reduced tidal asymmetry and reduced spring-neap tidal variations) and tidal stream energy sites in western Brittany and North Scotland (which were characterized by higher variability in the available resource and appeared less attractive for energy conversion). In western Brittany and North Scotland, areas with reduced flood-ebb asymmetry were confined to the central divergence zone identified within the Fromveur Strait, the eastern parts of the Pentland Firth and from the Fall of Warness to the Westray Firth (Orkney). Sites with reduced spring-neap variability were only identified in the centre of the Fromveur Strait, increasing its attractiveness for energy conversion.

(v) Increased variability may arise from the superimposed effects of wind-generated surface-gravity waves, with a reduction of the available mean spring tidal stream potential of the Fromveur Strait by around 12% during storm conditions. More significant effects were expected in the Pentland Firth, characterized by a strong exposure to North-Atlantic incoming waves aligned with the tidal currents.

Analysis of the temporal variability of the available resource is fundamental to optimise the design and location of kinetic energy converters. Our results, at high-spatial resolution, demonstrate the desirable characteristics of the tidal kinetic energy resource of the Alderney

Race, which had low tidal asymmetry and reduced spring-neap variability. Although no devices have yet been installed here, the Alderney Race has clear potential for large-scale exploitation of the tidal stream energy resource. Additional simulations, coupling waves and tidal circulation models in the western English Channel, will help to further characterize the temporal variability of the resource in more detail.

Data Accessibility. Results from the tidal harmonic analysis of numerical simulations will be made available and deposited in repository of Dryad (https://doi.org/10.5061/dryad.zw3r22853).

Authors' Contributions. NG conducted tidal simulations in western Brittany, performed the tidal analysis and predictions, and wrote the draft of the manuscript. SN conducted tidal simulations in North Scotland and wave predictions in the three computational domains, and reviewed the manuscript. JT conducted tidal simulations in the western English Channel and reviewed the manuscript. All authors approved the manuscript.

Competing Interests. The authors declare that they have no competing interests.

Acknowledgements. The present paper is a contribution to the research programme DIADEME ("Design et InterActions des Dispositifs d'extraction d'Energies Marines avec l'Environnement") of the Laboratory of Coastal Engineering and Environment (Cerema, http://www.cerema.fr). SN acknowledges the support of Supercomputing Wales (part-funded by the European Regional Development Fund, ERDF) which was used to run the wave model simulations. The contribution of JT was performed as part of the research program OceanQuest funded by ADEME.

References

1. Ocean Energy Europe. 2017 Ocean energy project spotlight - Investing in tidal and wave energy. Technical report OEE.
2. Lewis M, Neill S, Robins P, Hashemi M. 2015 Resource assessment for future generations of tidal-stream energy arrays. *Energy* **83**, 403–415.
3. Neill S, Hashemi M, Lewis M. 2014 The role of tidal asymmetry in characterizing the tidal energy resource of Orkney. *Renewable Energy* **68**, 337–350.
4. Michelet N, Guillou N, Chapalain G, Thiébot J, Guillou S, Brown AJG, Neill SP. 2019 Three-dimensional modelling of turbine wake interactions at a tidal stream energy site. *Applied Ocean Research* **95**, 102009.
5. Robins P, Neill S, Lewis M, Ward S. 2015 Characterising the spatial and temporal variability of the tidal-stream energy resource over the northwest European shelf seas. *Applied Energy* **147**, 510–522.
6. Guillou N, Neill SP, Robins PE. 2018 Characterising the tidal stream power resource around France using a high-resolution harmonic database. *Renewable Energy* **123**, 706–718.
7. Lewis M, Neill S, Hashemi M, Reza M. 2014 Realistic wave conditions and their influence on quantifying the tidal stream energy resource. *Applied Energy* **136**, 495–508.
8. Hashemi M, Neill S, Robins P, Davies A, Lewis M. 2015 Effect of waves on the tidal energy resource at a planned tidal stream array. *Renewable Energy* **75**, 626–639.
9. Guillou N, Chapalain G, Neill SP. 2016 The influence of waves on the tidal kinetic energy resource at a tidal stream energy site. *Applied Energy* **180**, 402–415.
10. Neill S, Hashemi M, Lewis M. 2014 Optimal phasing of the European tidal stream resource using the greedy algorithm with penalty function. *Energy* **73**, 997–1006.
11. Coles D, Blunden L, Bahaj A. 2015 Energy extraction potential from the Alderney Race. In *11th European Wave and Tidal Energy Conference* pp. 08D4–1–1–9 Nantes, France.
12. Neill S, Hashemi M, Lewis M. 2016 Tidal energy leasing and tidal phasing. *Renewable Energy* **85**, 580–587.
13. EMEC. 2020 The European Marine Energy Centre LTD. http://www.emec.org.uk.
14. Lewis M, McNaughton J, Márquez-Dominguez C, Tdeschini G, Togneri M, Masters I, Allmark M, Stallard T, Neill S, Goward-Brown A, Robins P. 2019 Power variability of tidal-stream energy and implications for electricity supply. *Energy* **183**, 1061–1074.
15. Myers L, Bahaj A. 2005 Simulated electrical power potential harnessed by marine current turbine arrays in the Alderney Race. *Renewable Energy* **30**, 1713–1731.
16. Neill S, Jordan J, Couch S. 2012 Impact of tidal energy convertor (TEC) arrays on the dynamics of headland sand banks. *Renewable Energy* **37**, 387–397.

17. Neill S, Litt E, Couch S, Davies A. 2009 The impact of tidal stream turbines on large-scale sediment dynamics. *Renewable Energy* **34**, 2803–2812.
18. Codiga D. 2011 Unified Tidal Analysis and Prediction Using the UTide Matlab Functions. Technical Report Graduate School of Oceanography, University of Rhode Island, Narragansett, RI.
19. Tawil T, Guillou N, Charpentier JF, Benbouzid M. 2019 On Tidal Current Velocity Vector Time Series Prediction: A Comparative Study for a French High Tidal Energy Potential Site. *Journal of Marine Science and Engineering* **7**.
20. SHOM. 2018 Sedimentological cartography. https://datashom.fr.
21. Thiébot J, Guillou N, Guillou S, Good A, Lewis M. in press Wake field study of tidal turbines under realistic flow conditions. *Renewable Energy*.
22. SHOM. 2000 Courants de marée et hauteurs d'eau. La Manche de Dunkerque à Brest. Technical Report 564-UJA Service Hydrographique et Océanographique de la Marine.
23. Hamdi A. 2007 French marine landscapes maps. Technical report Ifremer.
24. Guillou N, Thiébot J. 2016 The impact of seabed rock roughness on tidal stream power extraction. *Energy* **112**, 762–773.
25. SHOM. 2016 Courants de marée - Mer d'Iroise de l'île Vierge à la pointe de Penmarc'h. Technical Report 560-UJA Service Hydrographique et Océanographique de la Marine.
26. Fairley I, Masters I, Karunarathna H. 2015 The cumulative impact of tidal stream turbine arrays on sediment transport in the Pentland Firth. *Renewable Energy* **80**, 755–769.
27. Martin-Short R, Hill J, Kramer S, AVdis A, Allison P, Piggott M Tidal resource extraction in the Pentland Firth, UK: Potential impacts on flow regime and sediment transport in the Inner Sound of Stroma. *Renewable Energy* **76**.
28. Aurora. 2005 EMEC Tidal Test Facility Fall of Warness Eday, Orkney - Environmental Statement. Technical report Aurora Environmental Ltd.
29. Waggitt JJ, Cazenave PW, Torres R, Williamson BJ, Scott BE. 2016 Quantifying pursuit-diving seabirds' associations with fine-scale physical features in tidal stream environments. *Journal of Applied Ecology* **53**.
30. Easton M, Woolf D, Bowyer P. 2012 The dynamics of an energetic tidal channel, the Pentland Firth, Scotland. *Continental Shelf Research* **48**, 50–60.
31. Neill S, Vögler A, Goward-Brown A, Baston S, Lewis M, Gillibrand P, Waldman S, Woolf D. 2017 The wave and tidal resource of Scotland. *Renewable Energy* **114**, 3–17.
32. Kreitmar MJ, Adcock TAA, Borthwick AGL, Draper S, van den Bremer TS. 2020 The effect of bed roughness uncertainty on tidal stream power estimates for the Pentland Firth. *Royal Society Open Science* **7**.
33. Hervouet JM. 2007 *Hydrodynamics of free surface flows, modelling with the finite element method*. Cambridge: Cambridge University Press.
34. Thiébot J, Bailly du Bois P, Guillou S. 2015 Numerical modeling of the effect of tidal stream turbines on the hydrodynamics and the sediment transport - Application to the Alderney Race (Raz Blanchard), France. *Renewable Energy* **75**, 356–365.
35. Guillou N, Chapalain G. 2017 Tidal Turbines' Layout in a Stream with Asymmetry and Misalignment. *Energies* **10**, 1892.
36. Guillou N, Thiébot J, Chapalain G. 2019 Turbines' effects on water renewal within a marine tidal stream energy site. *Energy* **189**.
37. Vaslet D, Larsonneur C, Auffret JP. 1979 Les sédiments superficiels de la Manche 1/50000. Technical report Bureau de Recherches Géologiques et Minières - Centre National pour l'Exploitation des Océans.
38. Hamdi A, Vasquez M, Populus J. 2010 Cartographie des habitats physiques Eunis - Côtes de France. Technical Report DYNECO/AG/10-26/JP Ifremer.
39. Egbert G, Erofeeva SY, Ray R. 2010 Assimilation of altimetry data for nonlinear shallow-water tides: quarter diurnal tides of the Northwest European Shelf. *Continental Shelf Research* **30**, 668–679.
40. Shchepetkin AF, McWilliams JC. 2005 The regional oceanic modelling system (ROMS): a split-explicit, free-surface, topography-following-coordinate oceanic model. *Ocean Modelling* **9**, 347–404.
41. Umlauf L, Burchard H. 2003 Island wakes in shallow coastal water. *Journal of Geophysical Research: Atmospheres* **61**, 235–265.
42. Carrère L, Lyard F, Cancet M, Guillou A, Roblou L. 2012 FES 2012: A new global tidal model taking advantage of nearly 20 years of altimetry. In *Proceedings of meeting 20 Years of Altimetry*.

43. Guillou N, Chapalain G. 2017 Assessing the impact of tidal stream energy extraction on the Lagrangian circulation. *Applied Energy* **203**, 321–332.
44. Goward-Brown A, Neill S, Lewis M. 2017 Tidal energy extraction in three-dimensional ocean models. *Renewable Energy* **114**, 1–17.
45. Pingree RD, Griffiths DK. 1979 Sand transport paths around the British Isles resulting from M_2 and M_4 tidal interactions. *Journal of the Marine Biological Association of the United Kingdom* **59**, 497–513.
46. Friedrichs CT, Aubrey DG. 1988 Non-linear tidal distorsion in shallow well-mixed estuaries: a synthesis. *Estuarine, Coastal and Shelf Science* **27**, 521–545.
47. Pugh DT. 1987 *Tides, Surges and Mean Sea-Level*. Natural Environment Research Council, Swindon, UK: John Wiley & Sons.
48. Idier D, Paris F, Cozannet GL, Boulahya F, Dumas F. 2017 Sea-level rise impacts on the tides of the European Shelf. *Continental Shelf Research* **137**, 56–71.
49. Iyer AS, Couch SJ, Harrison GP, Wallace AR. 2013 Variability and phasing of tidal current energy around the United Kingdom. *Renewable Energy* **51**, 343–357.
50. Black and Veatch. 2011 UK tidal current resource and economics. Technical report Commissioned by the Carbon Trust and npower, Project number 121393.
51. Coles DS, Blunden LS, Bahaj AS. 2017 Assessment of the energy extraction potential at tidal sites around the Channel Islands. *Energy* **124**, 171–186.
52. Thiébaut M, Sentchev A. 2017 Asymmetry of tidal currents off the Western Brittany coast and assessment of tidal energy resource around Ushant Island. *Renewable Energy* **105**, 735–747.
53. Grant W, Madsen O. 1979 Combined wave and current interaction with a rough bottom. *Journal of Geophysical Research* **84**, 1797–1808.
54. Longuet-Higgins M, Stewart R. 1964 Radiation stresses in water waves; a physical discussion, with applications. *Deep-Sea Research* **11**, 529–562.
55. Neill S, Lewis M, Hashemi M, Slater E, Lawrence J, Spall S. 2014 Inter-annual and inter-seasonal variability of the Orkney wave power resource. *Applied Energy* **132**, 339–348.
56. Guillou N. 2017 Modelling effects of tidal currents on waves at a tidal stream energy site. *Renewable Energy* **114**, 180–190.
57. Hashemi M, Grilli S, Neill S. 2016 A simplified method to estimate tidal current effects on the ocean wave power resource. *Renewable Energy* **96**, 257–269.
58. Saruwatari A, Ingram D, Cradden L. 2013 Wave-current interaction effects on marine energy converters. *Ocean Engineering* **73**, 106–118.
59. Guillou N. 2014 Wave energy dissipation by bottom friction in the English Channel. *Ocean Engineering* **82**, 42–51.
60. Bennis AC, Furgerot L, Bois PBD, Dumas F, Odaka T, Lathuilière C, Filipot JF Numerical modelling of three-dimensional wave-current interactions in complex environment: Application to Alderney Race. *Applied Ocean Research* **95**.
61. Neill S, Hashemi M. 2013 Wave power variability over the northwest European shelf seas. *Applied Energy* **106**, 31–46.
62. Guillou N, Chapalain G. 2015 Numerical modelling of nearshore wave energy resource in the Sea of Iroise. *Renewable Energy* **83**, 942–953.